Biocarbon Production via Plasticized Biochar: Role of Feedstock, Water Content, Catalysts, and Reaction Time

Robert L. Johnson*[1], Kyle Castillo[1], Christian Castillo[1], Quang-Vu Bach[1], Cassidy Hihara[1], Liang Wang[2], Øyvind Skreiberg[2], Scott Q Turn[1]

[1] Hawaii Natural Energy Institute, University of Hawaii at Mānoa,

1680 East-West Rd., POST 109, Honolulu, Hawaii, 96822, USA

[2] SINTEF Energy Research, Sem Saelands vei 11, Trondheim, 7034, Norway

*Corresponding author email: robertlj@hawaii.edu

Abstract:

Studies into transient plastic phase biochar (TPPB) were conducted to compare how feedstock, moisture, acetic acid addition, and reaction time, impacted the formation of TPPB, and mechanical properties. Our results show that pyrolysis conditions sufficient for TPPB formation from birch wood, do not lead to TPPB formation from spruce, cellulose (paper plates), or rice straw. However, TPPB formation was possible with spruce and rice straw with the addition of water to the initial material. Plasticized and non-plasticized biochars (NTPPB) produced from spruce and rice straw were compared in terms of the charcoal yield, proximate analysis (fixed carbon content), and the mechanical properties of pelletized particles. Despite observing only minimal differences in the charcoal yields and fixed carbon contents between TPPB and (NTPPB) biochars, the tensile strengths of biochar and biocarbon pellets (calcined at 900 ^{o}C (N_2)) were substantially improved with TPPB. Biocarbon pellets produced from spruce-TPPB and rice straw-TPPB were 5x and 1.5x stronger than the NTPPB counterparts. Furthermore, adding +75 wt% H_2O resulted in biocarbon with nearly 10x's higher tensile strength despite both biocarbon materials being produced from a birch-TPPB precursor. Using birch we found that shorter reaction times also improved resulted in biocarbon pellets with nearly 3x higher tensile strength. Lastly, measured tensile (39 MPa) and compressive strength (188 MPa) values obtained from finely ground birch TPPB samples constitute one of the strongest biocarbon materials reported to date, and would have sufficient mechanical strength to serve as a direct substitute for petroleum carbon anodes without any binder. These results demonstrate that plasticized biochar can be produced from a variety of different feedstocks, and increasing the water content of the starting material, along with reducing the reaction time can be used to further improve the mechanical properties of the plasticized biochar for the formation of biocarbon.

Key Words: Transient plastic phase, decarbonization, metallurgic reductants, carbon anodes

Author Accepted Manuscript version of the paper by Robert L. Hohnson et al.
in Energy & Fuels, 37 (2023) Page 15808-15821,
http://dx.doi.org/10.1021/acs.energyfuels.3c01660

Introduction

One hundred ninety five nations have adopted the COP 21 Paris agreement to act to limit the increase in the average global temperature to less than 2 °C. Using biobased feedstocks to decarbonize industrial processes is one option to address this goal by reducing CO_2 emissions, while limiting impacts on industrial output. Aluminum production currently relies on fossil-derived carbon materials to manufacture anodes used in the process to reduce alumina (Al_2O_3) to aluminum. These carbon anodes are produced by mixing calcined pet-coke (85 wt%) with coal tar pitch (CTP) above the softening temperature of the CTP to form an anode paste. This paste is pressed into the desired shape to form a green anode and baked at 1200 ^oC.[1] Although CTP has favorable properties as a binder, it also has negative aspects related to its fossil carbon origin, availability of future supply, and poly-aromatic hydrocarbons (PAH) content and associated impacts on human health as a known carcinogen.[1] Aluminum anode requirements include very high fixed carbon content, low surface area, low O_2/CO_2 reactivity and compression strengths in the range of 20-40 MPa as determined via axial compression.[1, 2] Fossil coke is also used as a reductant in the submerged arc furnaces of the ferroalloy and silicomanganese industries with similar property requirements (tensile strength of 4 to 8 MPa).[3-5] Blast furnace cokes' tensile strengths range from 2.5 to 4.1 MPa with apparent densities of 0.744 to 0.859 kg/m^3.[6] Biobased substitutes for calcined pet-coke, CTP, and/or fossil reductants could contribute to reducing greenhouse gas emissions from the metallurgical industry. Directly substituting calcined pet-coke with biocarbon is problematic as the mechanical properties of biocarbon are very poor as compared to calcined pet coke. Substitution of CTP with bio-oil produced from fast pyrolysis has shown to be a viable substitute. Although, producing high quality bio-oil requires numerous processing steps and the total reduction in green house gas emissions is modest as the binder comprises only 15-25 wt% of the material. The greatest impact for reducing green house gas emissions requires processing technology to utilize biomass to produce the complete anode. Standard biomass carbonization proceeds via a charring (no molten phase) and not coking (molten phase) mechanism. The lack of a molten phase during carbonization results in the product retaining much of the morphological features of the parent material, and limits inter-and intra-particle bonding leading to high surface area, and poor mechanical properties and electrical properties.[7] Improved mechanical properties of biobased substitutes for calcined pet-coke, CTP, and/or fossil reductants are critical to their utilization as fossil replacements in the metallurgical industry.

Biomass pyrolysis to primarily produce solid carbonized products has been explored across a range of pressures, temperatures, heating rates, feedstocks, residence times, and reactive environments. [7] Product

Author Accepted Manuscript version of the paper by Robert L. Hohnson et al.
in Energy & Fuels, 37 (2023) Page 15808-15821,
http://dx.doi.org/10.1021/acs.energyfuels.3c01660

yields and distributions reflect the feedstock characteristics and severity of process conditions. Although, temperature is the key processing variable that dictates the extent of carbonization, with temperatures in excess of 800 °C required to form extended poly condensed aromatic sheets characteristic of a material with high fixed carbon content (> 85%) and low resistivity (<100 μΩ*m) need for aluminum electrolysis.[1] Altering the biomass to biocarbon processing pathway is a promising approach to alter the properties of the resultant materials, which is analogous to geochemical processes that yield a suite of different carbon products.

Under certain conditions, pressurized pyrolysis can produce a solid appearing to have experienced a molten phase. Table 1 summarizes process conditions and feedstock materials that include microcrystalline cellulose, [8, 9] birch,[10, 11] oak,[11] olive stones, [12] pine, [13] miscanthus, [13] corn stover, [13] lignin[13], cellulose, [13] and xylan.[13] This molten phase biochar product has been termed transient plastic phase biochar (TPPB). Researchers producing carbon foams using thermochemical conversion have also identified molten phase formation. Considering the huge volume of biomass thermochemical conversion literature over the past several decades, the formation of a molten phase is relatively unexplored.

Table 1. Conditions reported for molten biochar formation

Feedstock	Moisture Content (% wet basis)	Reaction Type	Pressure (MPa) Initial/Peak	Temperature (°C)
Microcrystalline cellulose[8]	4.7	Constant Volume	2.26/7.39	309
Microcrystalline cellulose[9]	0.0 to 6.0	Constant Volume	2.4/6.4 to 9.8 3.55/10.4 4.79/12.1	260 to 400 300 to 325 300
Birch[11]	7.9	Constant Volume	0.1/9.57	300
Oak[11]	7.5	Constant Volume	2.69/7.62	300 to 400
Birch[11]	8-10 %	Constant pressure	12.5	320
Olive stones[12]	not reported*	Constant pressure	1.0/1.0	Ramp to 500
*batch reactor contained 200 g of feedstock and 25 ml of liquid water to generate steam environment				

The underlying processes that result in the molten phase formation is still not fully understood. One explanation from cellulose experiments postulates that elevated pressure acts to partition feedstock

Author Accepted Manuscript version of the paper by Robert L. Hohnson et al.
in Energy & Fuels, 37 (2023) Page 15808-15821,
http://dx.doi.org/10.1021/acs.energyfuels.3c01660

devolatilization products directly to the liquid phase. When coupled with heating rates of 20-60 °C min^{-1}, the condensed volatiles formed a liquid phase intermediate prior to charcoal formation.[8, 9] This hypothesis is in agreement with temperatures (250 to 475 °C) where an "intermediate active cellulose" forms.[14] Lédé differentiates between bio-oils formed from condensed pyrolysis vapors and liquids that are solid at room temperature having gone through an intermediate active form.[14] Literature from carbon-foam research suggested that both heating rate and pressure were important for the formation of a molten phase. During pyrolysis, a large exotherm was identified that is postulated to be critical to the melting process.[12, 13] Molten product viscosity differences were suggested to reflect feedstock ash content.[13] Olive stones were pyrolyzed under 1 MPa N_2 and a 10 °C min^{-1} ramp to 500 °C with liquid water present in a 1 L reactor but separate from the feedstock.[12] Based on experimental results, it was concluded that in the early stages of heating, the partial pressure of water vapor increases, inhibiting dehydration reactions. At ~150 °C, biopolymers undergo endothermic scission to produce a "high viscosity melt" that undergoes exothermic dehydration. This heat release increases the sample heating rate, supporting further depolymerization while the reactor pressure maintains volatiles in the condensed phase. With increasing temperature, liquid volatiles boil or are thermally degraded and leave as gas, creating an expanded melt, increasing porosity, and a final carbon foam product. Suppressed dehydration reactions were postulated as the key difference between this process and conventional pyrolysis.

Recent constant pressure experiments studied the impact of pressure on TPPB formation. [15] Reactions with birch wood at 320 °C required pressure in excess of 10.4 MPa for complete molten phase formation. The water boiling point at this pressure is 270 °C and maintaining condensed water in the reactor was identified as critical to molten phase formation. Moreover, a reaction with 12.4 MPa pressure and 275 °C did not form a molten phase, suggesting that a minimum temperature between 275 and 320 °C is required. TPPB and non transient plastic phase biochar (NTPPB) produced across a range of pressures (0.1-12.4 MPa) showed no differences in solid yields, or the ^{13}C NMR spectra. This finding suggests that secondary char formation is not the critical mechanism for TPPB formation. The molten phase was confirmed using a reactor containing two sections separated by a 1 mm screen. 2 -4 mm birch particles loaded above the screen appeared as TPPB product below the screen at the test conclusion. This work postulated that sufficient pressure maintains water in the condensed phase favoring hydrolysis (equation 1) over condensation (equation 2), where C-O-C represents linkages between base units in biomass' polymeric structure. Hydrolysis and condensation reactions are reversible with H_2O being a reactant in hydrolysis, and a product in condensation. Therefore, if water is quickly evaporated from the system (as in the case for pyrolysis under standard pressure conditions) the removal of water will shift the reaction

Author Accepted Manuscript version of the paper by Robert L. Hohnson et al.
in Energy & Fuels, 37 (2023) Page 15808-15821,
http://dx.doi.org/10.1021/acs.energyfuels.3c01660

entirely in the direction of condensation. The smaller molecular weight fragments produced by hydrolysis form the molten phase that solidifies into TPPB upon cooling.

$$\text{C-O-C} + H_2O \rightarrow \text{C-OH} + \text{C-OH} \quad \text{“Hydrolysis”} \qquad (1)$$

$$\text{C-OH} + \text{C-OH} \rightarrow \text{C-O-C} + H_2O \quad \text{“Condensation”} \qquad (2)$$

Until recently, little attention was given to the mechanical properties of TPPB materials, and the potential utility to improve the mechanical strength of biochar and biocarbon. Recent work compared the mechanical performance of TPPB and (NTPPB) biochars produced from birch at 320 °C with powder compaction experiments. This methodology was adopted from pill making research conducted by the pharmaceutical industry and recognizes that the predominant factor resulting in strong pellets/tablets/pills is the capacity for the material to form strong inter particle and intra particle bonds by undergoing plastic deformation during compression. [16-18] Therefore the tensile strength of the pellets formed from particle compaction serves as an indirect measure or the material plasticity.[15] These results showed that birch TPPB materials display greater plasticity, reduced elasticity (volume expansion after 128 hours) and reduced thermal expansion.[15] Furthermore, calcined (N_2 900 °C) TPPB pellets produced transient plastic phase biocarbon (TPPC) pellets with tensile strength of 4.4 MPa and apparent density of 1.026 g/cm^3, exceeding requirements of blast furnace reductant cokes.[6] Additionally, the measured compression strength of TPPC pellets was 17± 1.7 MPa, comparable to the pellets of calcined pet-coke CTP mixtures.[1, 2, 15] The birch TPPB intermediate pellets were produced from relatively large particles (0.5-1.0 mm) without binder.

This initial work showed TPPB as a promising route to improve biocarbon mechanical properties. Further research is needed to understand how different feedstocks and process conditions impact molten phase/TPPB formation and mechanical properties of biocarbon products. The following objectives were identified to fill this knowledge gap and inform process design. The first objective was to determine if birch TPPB formation reaction conditions would produce similar results on other biomass feedstocks. A variety of biomass types, including: spruce (gymnosperm), rice straw (herbaceous high ash content), oak (angiosperm), Avicell, and cellulose plates, were tested to gain insight into how their differences would impact TPPB formation. The effects of feedstock moisture content and acetic acid addition on the formation of TPPB and the mechanical properties of the biochar and biocarbon pellets were also explored. The reaction time needed to produce TPPB and its influence on pellet mechanical properties was investigated. In order to investigate post TPPB formation process effects, an experiment was conducted

Author Accepted Manuscript version of the paper by Robert L. Hohnson et al.
in Energy & Fuels, 37 (2023) Page 15808-15821,
http://dx.doi.org/10.1021/acs.energyfuels.3c01660

where the reactor was depressurized while at reaction temperature. Lastly, biocarbon was formed from finely ground birch and spruce TPPB samples to provide insight into benefits derived from comminution.

Materials and Methods

Sample preparation

Norwegian spruce and birch stem woods (forest outside Trondhiem), rice straw obtained from freshly harvested fields in the Sacramento valley of northern California, oak (Conagra Corp), and paper plates (a cellulose proxy) were ground into <2 mm and <4 mm size fractions using a rotary knife mill (Fritsch Pulverisette 19, Idar-Oberstein, Germany), and size fractionated using a sieve shaker (Rotap RX-29, WS Tyler, Mentor, OH) for 5 minute intervals. Avicel (type PH-102) with a 90 µm average particle size was purchased from FMC Corporation and used as received.

Feedstock moisture contents (determined by drying overnight at 105 ^{o}C until constant weight) are reported on a wet basis. Water was added to feedstocks in equilibrium with ambient conditions (air dry) to produce samples with increased moisture content. The added water is reported relative to the air dry mass of feedstock ($mass_{H2O\ added}/mass_{biomass\ eq\ ambient}$). This value does not account for the equilibrium value of the parent biomass (~8% wet basis). The prescribed amounts of water and biomass were added to an empty reactor, sealed, and allowed to equilibrate overnight prior to pyrolysis tests.

Similarly, acetic acid was included in experiments at levels of 5 and 10% relative to the air dry mass of feedstock. When acetic acid and water were both added, the total liquid loading (mass of acetic acid plus mass of water) are reported relative to the air dry mass of feedstock.

Reactor design and testing

All pyrolysis tests used a wall heated tube bomb (WHTB) reactor system described previously.[15] After loading with biomass, the reactors were weighed, leak checked, purged, and pressurized using industrial nitrogen from a compressed gas cylinder. Purging was done under elevated pressure to minimize the water lost from the system. All tests were conducted under constant pressure (~12.4 MPa) controlled with a back pressure regulator. Upon heating the reactor in a nominally constant temperature sand bath, pretest N_2 and feedstock-derived gases expanded and were released through the back pressure regulator. This transient heating period produced a ~15% overshoot above the set point pressure while the system

Author Accepted Manuscript version of the paper by Robert L. Hohnson et al.
in Energy & Fuels, 37 (2023) Page 15808-15821,
http://dx.doi.org/10.1021/acs.energyfuels.3c01660

achieved equilibrium. Feedstocks and reactor conditions used in the test campaign are summarized in Table 2.

Author Accepted Manuscript version of the paper by Robert L. Hohnson et al.
in Energy & Fuels, 37 (2023) Page 15808-15821,
http://dx.doi.org/10.1021/acs.energyfuels.3c01660

Table 2: Summary of test conditions conducted at 320 °C and constant pressure of 12.4 MPa.

Test ID	Experiment Purpose	Biomass	Particle Size (mm)	Added H_2O (wt %)	Acetic Acid	Reaction time (min)
1	TPPB	Spruce	1-2	0 (AD) *	0	30
2	TPPB	Rice straw	1-2	0 (AD) *	0	30
3	TPPB	Oak	1-2	0 (AD) *	0	30
4	TPPB	Cellulose (fibers)	1-2	0 (AD) *	0	30
5	TPPB	Avicel	0.09	0 (AD) *	0	30
6	H_2O	Spruce	1-2	25	0	30
7	H_2O	Spruce	1-2	50	0	30
8	H_2O	Spruce	1-2	75	0	30
9	H_2O	Spruce	1-2	107 (sat)*	0	30
10	Acetic Acid	Spruce	1-2	45	5	30
11	Acetic Acid	Spruce	1-2	40	10	30
12	H_2O	Birch	1-2	50	0	30
13	H_2O	Birch	1-2	75	0	30
14	Time	Birch	1-2	25	0	10
15	Time/H_2O	Birch	1-2	25	0	30
16	Time	Birch	1-2	25	0	60
17	H_2O	Rice Straw	1-2	25	0	30
18	H_2O	Rice Straw	1-2	50	0	30
19	H_2O	Rice Straw	1-2	100	0	30
20	H_2O	Rice Straw	1-2	225	0	30
21	Pressure release	Birch	1-2	25	0	30

* Air dry (AD) moisture contents of spruce, rice straw, oak, cellulose (fibers), Avicel and birch used in Tests 1 to 21 were 8.3, 8.2, 8.0, 7.5, 7.9 and 8.1 wet basis, respectively.

*(sat) indicated the biomass is fully soaked with water

Author Accepted Manuscript version of the paper by Robert L. Hohnson et al.
in Energy & Fuels, 37 (2023) Page 15808-15821,
http://dx.doi.org/10.1021/acs.energyfuels.3c01660

Proximate analysis

Moisture content, volatile matter, fixed carbon and ash of the biochars produced from the WHTB reactor were determined using a LECO TGA801 System (LECO Corporation, St. Joseph, MI) with operating conditions as specified by the manufacturer for proximate analysis. The LECO TGA 801 program is described previously.[15] All samples were run in triplicate with ~1 g of sample used for each replicate. Averages and standard deviations are reported.

Pellet preparation and testing

Biomass and biochar compaction experiments were conducted with a universal tester (Shimadzu, model AGS-X) controlled by Trapezium software (version 1.5.6) and equipped with a 5 kN load cell (±1% from 10-5000 N). Pellets were formed from biochar particles ranging in size from 0.5 to 1.0 mm under 88 MPa pressure using a 6 mm diameter die (Precision Elements Ltd, Traverse City, MI) made from D2 tool steel. The same apparatus was used to produce pellets from biomass and biochar with 168 MPa of pressure.

Tensile strength, determined using diametric compression of cylindrical pellets with a piston travel speed of 1 mm/min, was calculated using equation (3), where σ_T is tensile strength (MPa), F_{max} is the maximum measured force (MN), and D and H are the diameter (m) and height (m) of the pellet, respectively. Tensile strength of pellets is commonly determined by compressive loading transverse to the cylinder axis, although true tensile strength is often underreported from excessive strain at the points of contact.[19]

$$\sigma_T = \frac{2F_{max}}{\pi DH} \quad (3)$$

Apparent density, ρ, (kg/m^3) was calculated using the oven dry mass, m (kg), of the pellet as shown in equation (4). Pellet dimensions were determined with a micrometer.

$$\rho = \frac{m}{\pi\left(D/2\right)^2 H} \quad (4)$$

Compression strength , σ_C, (MPa), was determined by axially compressing the pellets until failure and calculated using equation (5).

$$\sigma_C = \frac{F_{max}}{\pi\left(D/2\right)^2} \quad (5)$$

Author Accepted Manuscript version of the paper by Robert L. Hohnson et al.
in Energy & Fuels, 37 (2023) Page 15808-15821,
http://dx.doi.org/10.1021/acs.energyfuels.3c01660

Determination of water holding capacity of feedstock

The water holding capacity of feedstocks were determined by placing 10 g of 1-2 mm particles in 500 ml of DI water and mixing for 2 hrs. The hydrated materials were vacuum filtered for 15 minutes after all additional water was pulled through the filter.

Calcination of biomass and biochar pellets to produce biocarbon pellets

Biomass and biochar pellets were first weighed, then devolatilized in a 25 mm quartz tube furnace using a temperature ramp rate of 1 °C/min to 900 °C. After holding for 1 hr, samples were passively cooled. The quartz tube was purged and calcination was conducted under a flow of 1.6 L nitrogen /min (Matheson Tri-Gas, 99.999% purity) that passed through a trap (Restek, RES-20601) to reduce oxygen below 20 ppb. Pellet mass was determined following devolatilization and dimensions were measured using a micrometer (Mintoya Corp., Model CD-6”C, ±5 μm). Samples were run in duplicate and values reported are the average.

Size reduction of TPPB materials

TPPB materials were ground into a fine powder using a Retsch cryomill. The materials were milled using two 2-minute cycles with a 20 hz frequency. The materials were pre-cooled for 3 minutes and for 2 minutes between milling periods.

Thermogravnimetric Analysis (TGA)

Thermogravnimetric analysis was carried out using a Perkin Elmer TGA8000 with Pyris software (version 13.3.3.0032, 2016. Materials were cryo-milled into a fine powder prior to TGA analysis. Thermograms were acquired using a 10 ^{o}C/min ramp to 1100 ^{o}C including a 30 minute hold period at 110 ^{o}C under UHP nitrogen min (Matheson Tri-Gas, 99.999% purity) with a sample flow rate of 20 ml/min, and a balance flow rate of 40 ml/min.

Author Accepted Manuscript version of the paper by Robert L. Hohnson et al.
in Energy & Fuels, 37 (2023) Page 15808-15821,
http://dx.doi.org/10.1021/acs.energyfuels.3c01660

Raman Spectroscopy

Raman spectra were aquired using a DXRxi Raman Imaging Microscope with 100x magnification objective lens with excitation using a 532 nm laser. Samples were mounted on the cylindrical axis onto a glass slide under the Raman microscope and focused using the objective lens. The laser was powered to 1.5 – 2 mW for a 0.5-1 second exposure time with 1000 scans. The spectra were analyzed utilizing the Omnic xi software. The area under the curve was determined by the Omnic xi area measurement tool. Raman spectroscopy was carried out on the calcined samples of birch and spruce obtained from the cryomilled materials.

Equilibrium analysis of rice straw

FactSage™ version 8.0 software was used to calculate the thermochemical equilibrium product distribution for constant volume carbonization of rice straw at 320 °C. Reactant ratios for rice straw based on ultimate and X-ray fluorescence analyses are presented in Table 3. Case 1 presents element ratios based on 100 g of rice straw at 8% moisture content (wet basis), i.e. 92% rice straw dry matter and 8% water. Cases 2 to 9 are based on the Case 1 data with the addition of water as a percentage (ranging from 10% to 40%) of the Case 1 feedstock (92% dry matter and 8% water) mass. For example, reactant masses for Case 5 are based on 92 g rice straw dry matter and 8+24=32 g H_2O. The equilibrium product distribution was calculated using the reactant ratios in Table 3, a constant reactor volume of 900 mL, and a product temperature of 320 °C.

Table 3. Feedstock element ratios for constant volume carbonization of rice straw with varied moisture contents.

Case	1	2	3	4	5	6	7	8	9
Added H_2O (% of fuel mass at 8% H_2O)	0	10	20	22	24	26	28	30	40
Fuel Moisture Content (%)	8	8	8	8	8	8	8	8	8
Element composition (%)									
C	34.457	31.325	28.714	28.244	27.788	27.347	26.920	26.506	24.612
H	5.418	5.936	6.367	6.445	6.520	6.593	6.664	6.732	7.045
N	0.640	0.582	0.533	0.525	0.516	0.508	0.500	0.492	0.457

Author Accepted Manuscript version of the paper by Robert L. Hohnson et al.
in Energy & Fuels, 37 (2023) Page 15808-15821,
http://dx.doi.org/10.1021/acs.energyfuels.3c01660

S	0.077	0.070	0.064	0.063	0.062	0.061	0.060	0.059	0.055
O (by difference)	49.154	52.766	55.776	56.319	56.844	57.353	57.846	58.323	60.507
Cl	0.372	0.338	0.310	0.305	0.300	0.295	0.291	0.286	0.266
F	0.027	0.025	0.023	0.022	0.022	0.021	0.021	0.021	0.019
Na	0.015	0.014	0.013	0.012	0.012	0.012	0.012	0.012	0.011
Mg	0.079	0.072	0.066	0.065	0.064	0.063	0.062	0.061	0.056
Al	0.029	0.026	0.024	0.024	0.023	0.023	0.023	0.022	0.021
Si	5.617	5.106	4.681	4.604	4.530	4.458	4.388	4.321	4.012
P	0.061	0.055	0.051	0.050	0.049	0.048	0.048	0.047	0.044
Cl	0.372	0.338	0.310	0.305	0.300	0.295	0.291	0.286	0.266
K	3.062	2.784	2.552	2.510	2.469	2.430	2.392	2.355	2.187
Ca	0.281	0.255	0.234	0.230	0.227	0.223	0.220	0.216	0.201
Mn	0.102	0.093	0.085	0.084	0.082	0.081	0.080	0.078	0.073
Fe	0.101	0.092	0.084	0.083	0.081	0.080	0.079	0.078	0.072
Cu	0.005	0.005	0.004	0.004	0.004	0.004	0.004	0.004	0.004
Br	0.026	0.023	0.021	0.021	0.021	0.020	0.020	0.020	0.018
Rb	0.005	0.005	0.004	0.004	0.004	0.004	0.004	0.004	0.004
Mo	0.023	0.021	0.019	0.019	0.019	0.018	0.018	0.018	0.016

Results and Discussion

Additional feedstock testing using TPPB conditions (birch feedstock)

The TPPB formation process was explored using different biomass materials and reactor conditions which formed TPPB from birch stem wood. The following materials were tested: spruce (gymnosperms), oak (angiosperms), rice straw (grassy high ash), paper plates (cellulose fibers), and Avicel (microcrystalline cellulose). Proximate analysis data shown in Table 4 are consistent with expected values for these materials.

Table 4: Proximate analysis (dry basis) for feedstock materials used in this study

Feedstock	Fixed carbon (wt%)	Volatile matter (wt%)	Ash (wt%)
Birch	15.87	83.86	0.28
Spruce	17.43	82.34	0.23
Rice Straw	15.68	67.27	17.05
Oak	17.99	79.39	2.42

Author Accepted Manuscript version of the paper by Robert L. Hohnson et al.
in Energy & Fuels, 37 (2023) Page 15808-15821,
http://dx.doi.org/10.1021/acs.energyfuels.3c01660

Cellulose	11.62	86.78	1.60
Avicel	12.05	88.06	0

This set of biomass materials with different physio-chemical properties, was chosen to aid in identifying critical factors for TPPB formation. Table 5 shows values for cellulose, hemicellulose, lignin and ash contents of the feedstocks reported in literature. Test results under identical reactor conditions (Table 6) show that birch, oak and Avicel formed TPPB (Table 1, Test IDs 3&5), but spruce, rice straw, and cellulose fibers (IDs 1, 2, 4) did not. Differences in the TPPB formation could result from differences in the lignin content and composition between these materials. The lignin makeup of angiosperms and gymnosperms differ: (1) angiosperms having significant amounts of acid soluble lignin and higher fractions of lignin monomers that contain syringyl base units (di-methoxy phenyl propane units),[20] (2) lignin isolated from softwood and hardwood biomass using the Lignoforce™ process showed hardwood species had a reduced average molecular weight, and reduced glass transition temperature,[21 20] and (3) angiosperms contain a higher fraction of acylated carbohydrates in their hemicellulose compared to gymnosperms.[22] Reduced average molecular weights of lignin components (e.g. 5,426 g/mol for hardwood vs 12,926 g/mol for softwood[20]) serve to lower their glass transition temperatures (132 °C hardwood vs 177 °C softwood).[20]

TPPB readily formed with microcrystalline cellulose but not cellulose fiber. Microcrystalline cellulose would be expected to comprise smaller average molecular weight components. Rice straw did not form TPPB and its high ash content likely plays a role by binding water via hydrolysis of SiO_2 (see equilibrium analysis below).

Table 5: Summative analysis of various feedstocks

Feedstock	Cellulose	Hemicellulose	Lignin – acid insoluble	Lignin – acid soluble
Rice straw[23]	36.32[a]	19.45[b]	14.07	3.53
Spruce[22]	40.1	20.3	31.1	0.35
Birch[22]	38.6	24.2	19.5	17.3
Oak[24]	34.5	18.6	28.0[c]	

[a] reported as glucose
[b] reported as xylose
[c] reported as Klason lignin

Author Accepted Manuscript version of the paper by Robert L. Hohnson et al.
in Energy & Fuels, 37 (2023) Page 15808-15821,
http://dx.doi.org/10.1021/acs.energyfuels.3c01660

The lack of molten phase formation with spruce and rice straw is different than Stahfeld's results reporting molten phase formation with pine (softwood) and corn stover (grass).[13] Carbon dioxide was used at 10.4 MPa and a final temperature of 510 °C, supercritical conditions where it would behave like a hydrophobic solvent.[25] This could partition water to interact with the more hydrophilic biomass leading to greater reactivity. This partitioning influence was demonstrated using acid catalyzed (hydronium mediated) reactions run in polar aprotic solvents and resulted in reaction rates increasing dramatically.[26, 27]

Table 6: Summary of TPPB occurrence for various feedstocks. (12.4 MPa, 320 °C, 30 min)

Material	**TPPB**
Birch[15]	Yes
Oak	Yes
Spruce	No
Rice Straw	No
Avicel	Yes
Cellulose Plates	Partial

Direct biocarbon production from various feedstocks

Tests were conducted to compare properties of biocarbon produced directly from the parent feedstock. Results (summarized in Table 7) confirm that biocarbon produced directly from biomass feedstock pellets result in biocarbon without appreciable mechanical strength. Biocarbon from birch showed very low apparent density (0.35 g/cc) and tensile strength that was below the load cell detection limit (5 N). Biocarbon pellets produced from rice straw broke apart from handling with forceps. Biocarbon pellets produced from spruce had the highest density (0.55 g/cc) and tensile strength (0.29 MPa) compared to rice straw or birch biocarbon pellets. Biocarbon produced from cellulose fibers had comparable density (0.59 g/cc) to spruce with significantly improved tensile strength (1.69 MPa). The biocarbon pellet formed from Avicel had nearly twice the density (1.07 g/cc) and more than five times the tensile strength (11.26 MPa) of all other materials. Differences in mechanical properties of the biocarbons directly produced from biomass pellets can be explained by several factors. First, Avicel is chemically processed material and has a lower degree of polymerization and lower average molecular weight compared to biomass or cellulose fibers.[28] The reduced molecular weight results in a reduced glass transition temperature and allows for a molten phase[14] during carbonization and forms strong covalent linkages between particles. Second, unlike the other materials (0.5 to 1 mm particles), Avicel is a fine powder (average particle size 90 µm) that can be more effectively compacted during the initial pellet formation (initial density 1.32 g/cc).

Author Accepted Manuscript version of the paper by Robert L. Hohnson et al.
in Energy & Fuels, 37 (2023) Page 15808-15821,
http://dx.doi.org/10.1021/acs.energyfuels.3c01660

Microcrystalline cellulose is commonly used as a binder for pills in the pharmaceutical industry as it has good plasticity and forms strong tablets.[18]

Table 7: Apparent density of biomass pellets and tensile strength and apparent density of biocarbon pellets formed by calcining biomass pellets at 900 °C.

Parent Material	Apparent density of biomass pellet (g/cc)	Tensile strength of bicarbon pellet (MPa)	Apparent density of biocarbon pellet (g/cc)	Yield (g biocarbon/g biomass)
Birch	0.911	NA	0.35	0.20
Spruce	0.962	0.29	0.55	0.23
Rice Straw	0.914	NA	NA	0.39
Avicel	1.32	11.26	1.07	0.23
Cellulose (plates)	1.15	1.69	0.59	0.20

Determination of water holding capacity

The water holding capacity for each feedstock was determined to provide an upper bound on the experimental range of tests exploring the effect of moisture content on the occurence of TPPB formation and biochar mechanical properties. (Table 8) Birch, spruce, rice straw and Avicell water holding capacities were 79.6, 107.5, 342 and 53.5 %, respectively. These values reflect differences in the materials apparent densities and available pore space. The cellulose plates were not included as soaking in water resulted in a breakdown of their general material structure. The water holding capacity provides a basic measure of the available space in the biomass material for water. The extent to which water will react with the biomass surface depends on ratio of biomass surface area and the total volume which water is able to freely diffuse. If the ratio of biomass/H_2O is constant, but the volume with which H_2O is able to diffuse is increased, the effect would be a reduced number of impacts between H_2O and biomass, resulting in a lower reaction rate. Therefore, normalizing the H_2O wt% to the void volume as determined by the water holding capacity provides a more accurate basis for the impact of water on the formation of TPPB.

Table 8: Water holding capacity of spruce, rice straw and birch

Biomass	Saturated H_2O %
Spruce	107.5
Birch	79.6
Rice Straw	342.5
Avicell	53.5

Author Accepted Manuscript version of the paper by Robert L. Hohnson et al.
in Energy & Fuels, 37 (2023) Page 15808-15821,
http://dx.doi.org/10.1021/acs.energyfuels.3c01660

Moisture content and TPPB/TPPC properties for birch

A series of tests were conducted to determine the effects of birch feedstock moisture content on biochar properties. Birch constant pressure reactions with added moisture of 25, 50, and 75 wt% of feedstock mass (at 8% equilibrium moisture content) were conducted for 30 mins at 320 ^{o}C and 12.4 MPa. All reactor conditions resulted in the formation of TPPB. Tensile strengths of the TPPB and TPPC formed from 0.5-1.0 mm TPPB particles are shown in Figure 1. TPPB pellet strengths ranged from 0.10 to 0.38 MPa and increased with increasing moisture content. TPPC pellets had tensile strengths of 1.9 to 6.8 MPa across the range of birch feedstock moisture contents of 25 and 75 wt% H_2O (Figure 1B).

The tensile strength of the TPPB pellets is strongly correlated to the plasticity of the particles that are being compressed into pellets.[16, 18] The strength of the calcined pellets (TPPC) reflects the capacity of the material to form inter and intra particle bonds during devolatilization. The formation of strong bonds between particles requires the materials experience a glass transition phase. Goring demonstrated that increased water content (~7 to 19% wet basis) of lignin and hemicellulose (xylan and glucomannan) samples reduced glass transition temperatures by 54 to 77 °C and ~120 °C, respectively. Water's role was to act as low molecular weight diluent that lowered the glass transition temperature by plasticizing the molecular chains of these amorphous polymers. Cellulose did not exhibit similar behavior and this was attributed to its high crystallinity. Bond strengths of wet lignin and wet hemicellulose were higher than their dry counterparts, with marked increases as the bond formation temperatures exceeded the glass transition temperature. The observed increase in the tensile strength of the calcined materials with increasing water content of biomass in the biochar formation step suggests that bond formation and/or bond strength between particles are enhanced. Water mediated hydrolytic cleavage produces polymeric fragments with reduced average molecular weight resulting in a reduced glass transition temperature and more available sites for bonding with neighboring particles.

Apparent density values for the samples (Figure 1C) show little variation between TPPB and TPPC pellets, indicating that the fraction mass loss incurred during calcination was accompanied by an equal fractional loss in volume due to pellet shrinkage. Fixed carbon content for the biochar samples are in a narrow range from 46 to 50% (see IDs 12,13,15 to x in Table S1), and this fraction remains after devolatilization to produce biocarbon. The apparent density being unchanged while the strength increases could suggest that although the bonding strength between particles is increasing, the basic structures of the particles is

Author Accepted Manuscript version of the paper by Robert L. Hohnson et al.
in Energy & Fuels, 37 (2023) Page 15808-15821,
http://dx.doi.org/10.1021/acs.energyfuels.3c01660

not significantly altered. This could reflect a lower average molecular weight of basic units, resulting in more “hanging bonds” that are available to form covalent linkages between particles.

The role of water in this system leads to some interesting questions with regards to the formation of TPPB. While the mechanical properties improve monotonically with water addition up to the fiber saturation point, the formation of TPPB does not require additional water be added to the materials. This suggests that hydrothermal reactions play a key role in the melting process, but TPPB is distinctly different than hydrochar.

Author Accepted Manuscript version of the paper by Robert L. Hohnson et al.
in Energy & Fuels, 37 (2023) Page 15808-15821,
http://dx.doi.org/10.1021/acs.energyfuels.3c01660

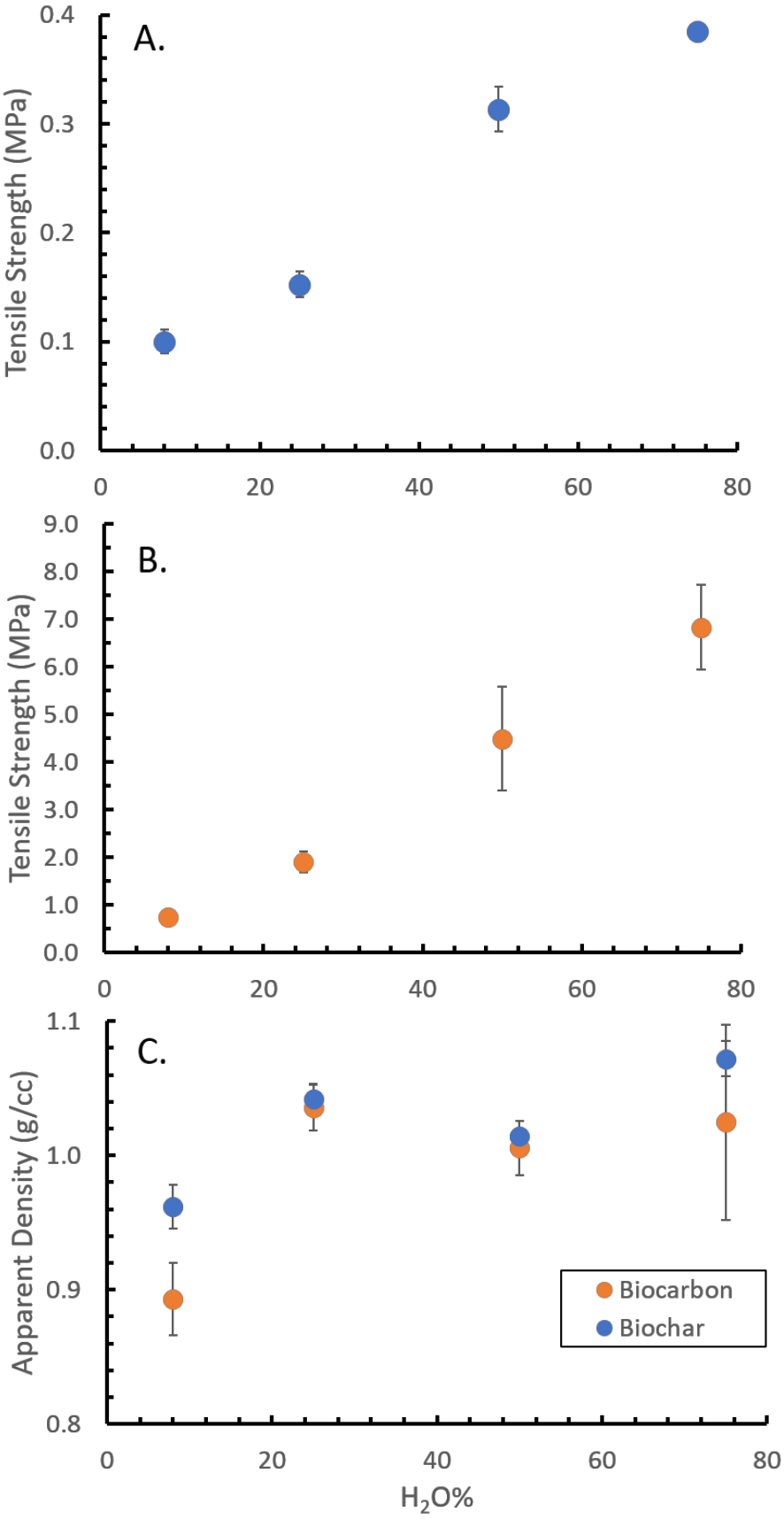

Author Accepted Manuscript version of the paper by Robert L. Hohnson et al.
in Energy & Fuels, 37 (2023) Page 15808-15821,
http://dx.doi.org/10.1021/acs.energyfuels.3c01660

Figure 1: Biochar (6 mm diameter, 88 MPa pressure) and biocarbon (6 mm diameter, 168 MPa pressure) pellets produced from birch stem wood (1-2 mm particle size produced at 320 °C and 12.4 MPa for 30 min) with different moisture content: (A) Tensile strength as measured using diametric compression of TPPB pellets, (B) Tensile strength of the TPPC pellets following calcination (N_2) 900 °C, (C) Apparent density data for TPPB and TPPC pellets as functions of moisture content.

Reaction time and TPPB properties for birch

A series of tests were conducted using birch (1-2 mm particle size, 25% added H_2O reacted at 320 °C and 12.4 MPa) to determine the effect of reaction time on mechanical properties of biochar and to estimate how quickly TPPB is formed. Complete TPPB formation was observed in our "short reaction" (10 minute) suggesting that TPPB formation is quite rapid as the time needed to reach 320 °C is roughly seven minutes.[15] Furthermore, with TPPB formation occurred between 275-320 °C, and the time to reach 275 °C is approximately 5 minutes.[15] This implies that the observed TPPB in the 10 minutes reaction was above the critical temperature for approximately 5 minutes. The exothermic reactions during carbonization could contribute to the sample heating rate. Legarra et al. documented the appearance of an exotherm in the reactor at ~10 minutes under similar conditions.[11] Stahlfeld and Belmont reported the occurrence of exotherms that appeared earlier and at lower temperature and displayed sharper peaks as reactor pressure increased.[13] Stahlfeld and Belmont and Rios et al. theorized that the exothermic pyrolysis augmented the heating rate imposed by the experimental apparatus to create a molten phase.[12, 13]

Figures 2A and 2B show the tensile strengths for the TPPB and TPPC time series samples. The 10 minutes TPPB sample had the highest value (0.195 MPa) and values decreased asymptotically with longer reaction times (0.14 MPa at 60 min). The pyrolyzing sample undergoes a molten phase that forms early (<10 min), followed by repolymerization reactions resulting in material with decreased capacity to form strong inter and intra particle bonds as the time at 320 °C is extended. These modest differences (<0.07 MPa) in TPPB pellet tensile strength produced more pronounced differences in tensile strength of TPPC pellets. The 10 min sample values of 2.9 MPa were nearly three times the 60 min sample value of 1.05 MPa. Apparent densities of the TPPB and TPPC samples showed little difference across reaction times and between biochar and calcined pelleted samples.

Author Accepted Manuscript version of the paper by Robert L. Hohnson et al.
in Energy & Fuels, 37 (2023) Page 15808-15821,
http://dx.doi.org/10.1021/acs.energyfuels.3c01660

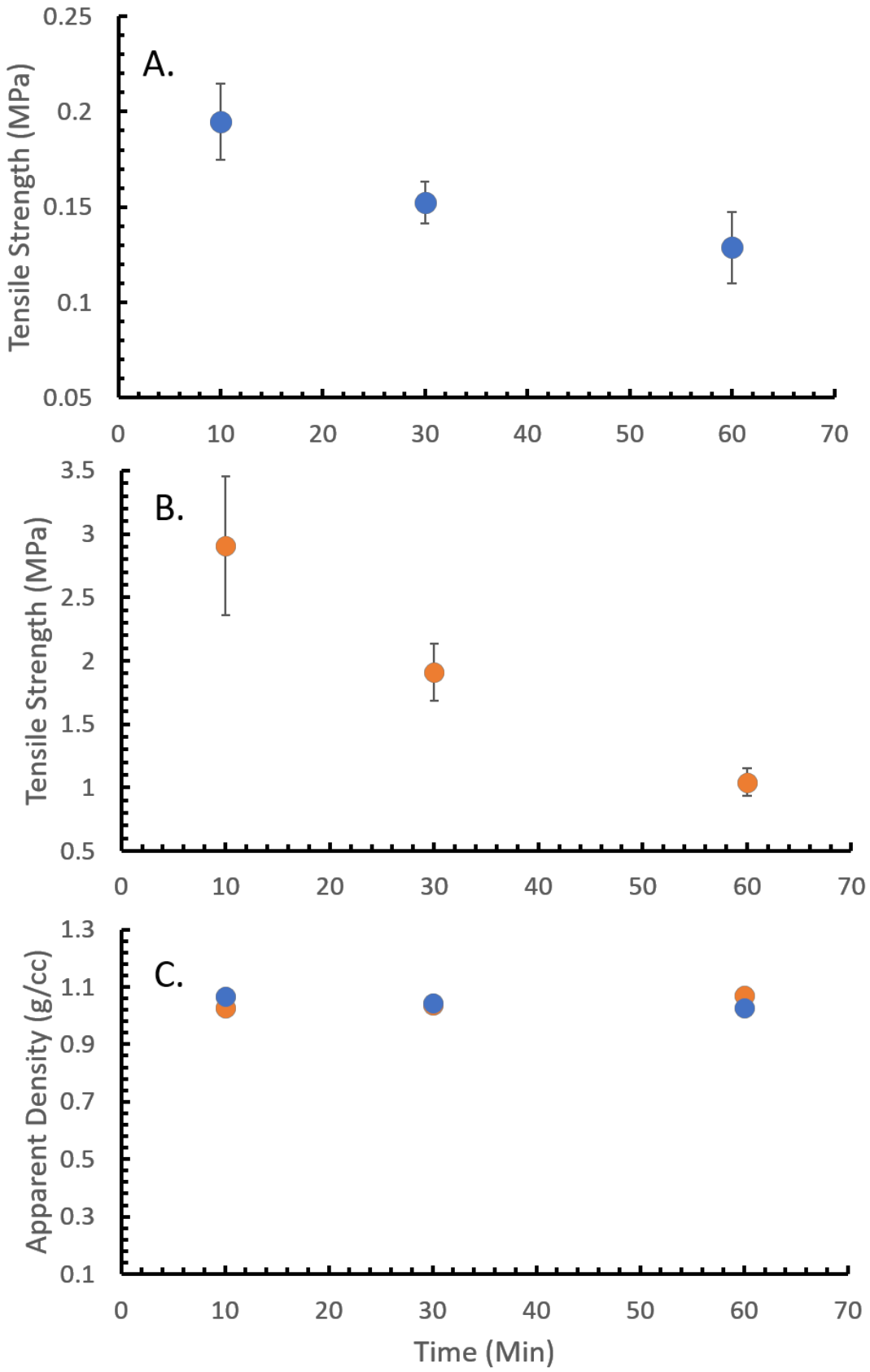

Author Accepted Manuscript version of the paper by Robert L. Hohnson et al.
in Energy & Fuels, 37 (2023) Page 15808-15821,
http://dx.doi.org/10.1021/acs.energyfuels.3c01660

Figure 2: Biochar (6 mm diameter, 88 MPa pressure) and biocarbon (6 mm diameter, 168 MPa pressure) pellets produced from birch stem wood (1-2 mm particle size, 25% added H_2O reacted at 320 ^oC and 12.4 MPa) for different reaction times: (A) Tensile strength as measured using diametric compression of TPPB pellets. (B) Tensile strength of calcined pellets, (C) Apparent density of biochar and biocarbon pellets.

Influence of moisture for TPPB formation using spruce

As spruce did not form TPPB under the same pressure/temperature/moisture conditions as was observed with birch, a series of tests (Table 2 Test IDs 6 to 9) were conducted to determine if increasing feedstock moisture content could induce the formation of TPPB. These experiments showed that TPPB could be formed with spruce, although added water was required. TPPB was only formed with addition of 75 and 107 (saturated) wt% H_2O but was not formed at 25 and 50 wt% water addition. Table S1 data show little difference in biochar yield (~60%) and fixed carbon content (~50% dry mass basis) for spruce across this span of moisture contents.

Figure 3 presents tensile strengths and apparent densities of biochar (blue circles) and biocarbon (orange circles) produced from spruce with different initial moisture contents. The tensile strengths of the NTPPB biochar pellets (25, 50 wt% H2O addition) were 0.144 and 0.136 MPa, respectively. As the tensile strength of a pellet reflects the plasticity of the compressed particles, this would indicate that this increase in feedstock water content had no appreciable impact. The addition of 75 wt% H_2O addition produce spruce char that had undergone a molten phase and the biochar pellet tensile strength increased to 0.35 MPa. A moisture content increase to 107 wt% H_2O addition (saturated fiber) nearly doubled the biochar tensile strength to ~ 0.7 MPa. The calcined materials exhibits a 5x increase in the tensile strength from 50 to 75 wt% H_2O addition but do not show further increase from 75 to 107 wt% H_2O.

The measured apparent density did not change significantly between the TPPB and NTPPB materials; all fell in a range from 0.88 to 1.00 g cm^{-3}. This is different than what was observed for birch where the TPPB pellet density was around 1.0 g/cc, and the NTPPB was significantly lower at 0.75 g/cc. Comparing the elasticities (defined as the pellet volume expansion after 128 hrs) of TPPB and NTPPB (Figure 3C) did not show a large difference with values ranging from 11-16 vol% expansion. This finding is unexpected as previous work with birch measured expansions of 17 and 4.3% for NTPPB and TPPB, respectively.[15] These data suggest that water-induced formation of spruce TPPB results in a material with significant differences compared to TPPB formed from birch.

Author Accepted Manuscript version of the paper by Robert L. Hohnson et al.
in Energy & Fuels, 37 (2023) Page 15808-15821,
http://dx.doi.org/10.1021/acs.energyfuels.3c01660

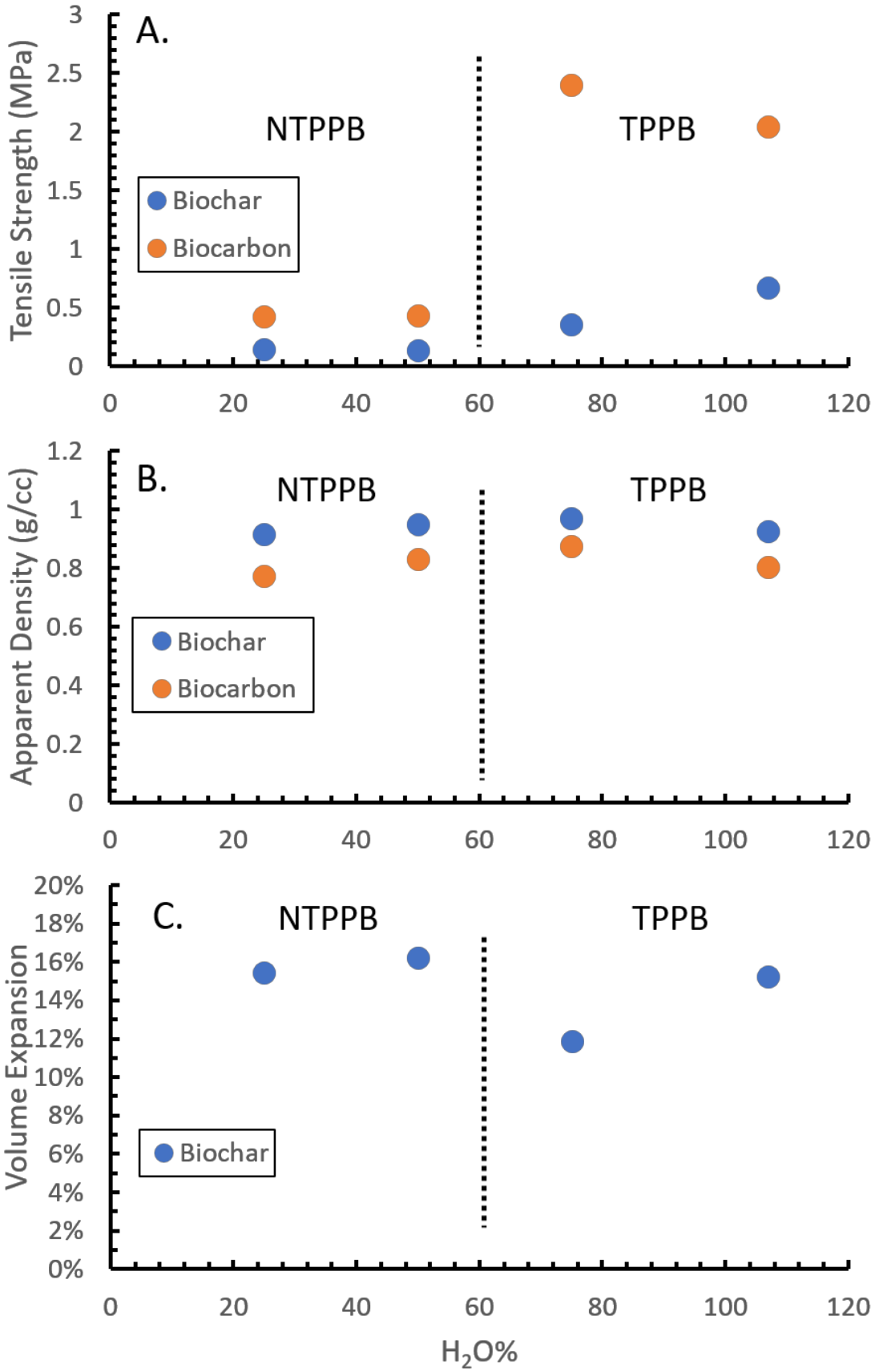

Author Accepted Manuscript version of the paper by Robert L. Hohnson et al.
in Energy & Fuels, 37 (2023) Page 15808-15821,
http://dx.doi.org/10.1021/acs.energyfuels.3c01660

Figure 3: Biochar (6 mm diameter, 88 MPa pressure) and biocarbon (6 mm diameter, 168 MPa pressure) pellets produced from spruce stem wood (1-2 mm particle size reacted at 320 °C and 12.4 MPa for 30 min) with different moisture content: (A) tensile strength measured using diametric compression, (B) apparent density and (C) elasticity measurements as measured by volume expansion after 128 hrs following compression at 168 MPa

Impact of acetic acid on TPPB formation in spruce

To investigate the differences observed with TPPB formation in spruce and birch a series of tests were conducted to probe this observation further. In addition to differences in lignin contents between birch and spruce, birch hemicellulose contains a significant fraction of acetylated sugars whereas spruce does not.[22,22] At temperatures around 200 °C the acetyl groups will fragment and form acetic acid and although acetic acid is considered a weak acid, catalytic activity for biomass hydrolysis reactions have been reported.[29] One potential hypothesis for the difference between TPPB formation in spruce and birch is that the acetic acid produced from the thermal break down of birch hemi-cellulose acts as a catalyst to form TPPB. This hypothesis was tested with a series of reactions using spruce and added acetic acid and H_2O. A 50 wt% H_2O addition condition was used as the baseline, as TPPB formation was not observed with water alone at this level. 5 and 10 wt% acetic acid levels were tested(). TPPB formation did not occur with either. These values of acetic acid loading would be quite high when compared to the acetic acid produced from TGA of birch, 2-3%.[22]

Figure 4 presents tensile strength and apparent density results for tests conducted with acetic acid addition. Biochar tensile strength displays only minor improvements with increasing acetic acid addition. Compared to the 0% acetic acid baseline (0.14±0.01 MPa) the 5 and 10 wt% acetic acid condition increased to 0.18±0.03 and 0.22±0.04 MPa. Compared to the fivefold increase produced by adding water (previous section) these are minor changes. A similar and modest change was also observed for biocarbon tensile strength, increasing from the 0.44 MPa baseline to 0.54 to 0.58 MPa with 5 and 10 wt% acetic acid addition.

Apparent density values were unchanged across the range of conditions presented in Figure 4B and are comparable to values in Figure 3B. The addition of acetic acid did not affect the volume expansion data presented in Figure 4C. Lastly, the biochar yield and fixed carbon content were not significantly affected by addition of water or acetic acid (Table S1).

Author Accepted Manuscript version of the paper by Robert L. Hohnson et al.
in Energy & Fuels, 37 (2023) Page 15808-15821,
http://dx.doi.org/10.1021/acs.energyfuels.3c01660

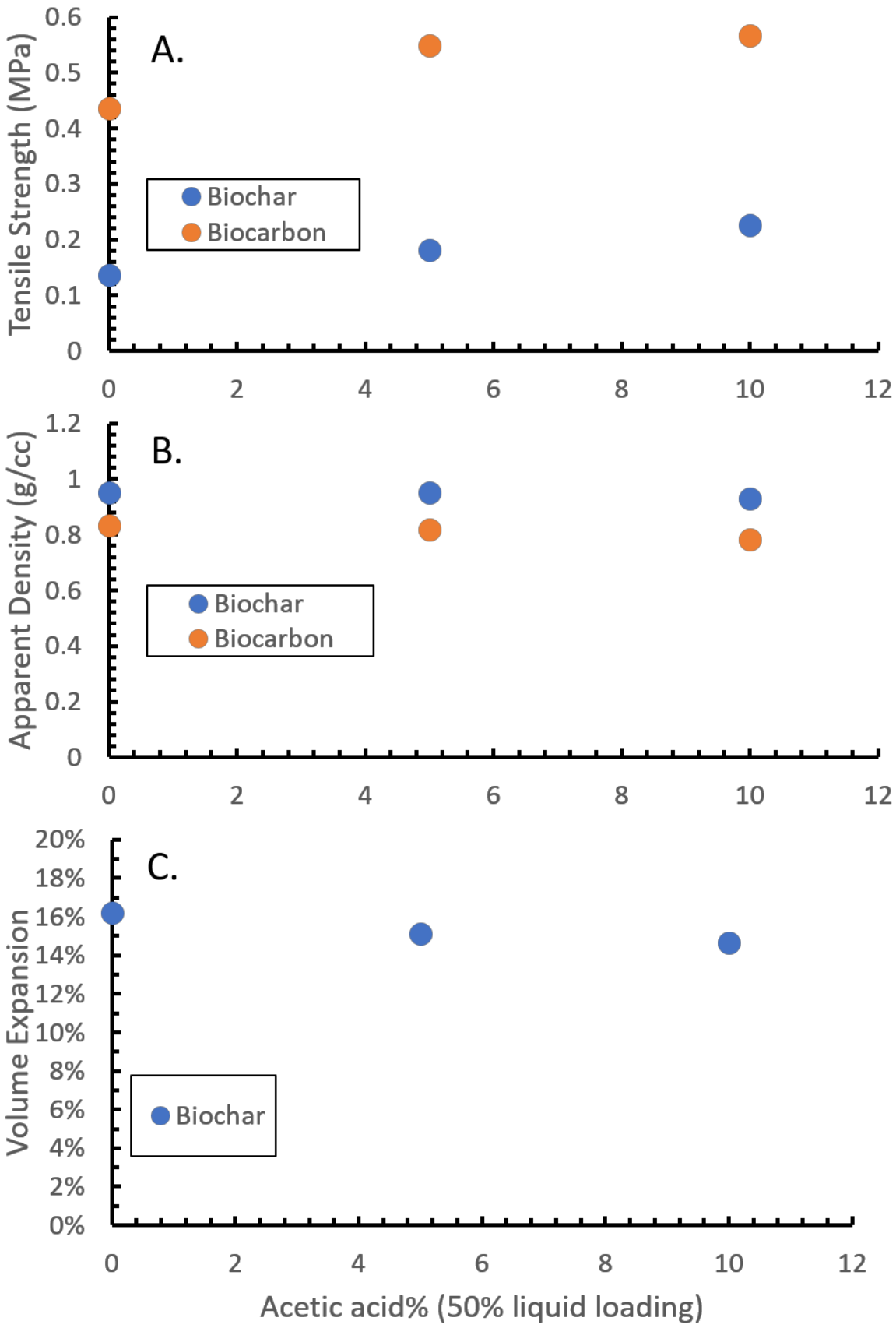

Author Accepted Manuscript version of the paper by Robert L. Hohnson et al.
in Energy & Fuels, 37 (2023) Page 15808-15821,
http://dx.doi.org/10.1021/acs.energyfuels.3c01660

Figure 4: Biochar (6 mm diameter, 88 MPa pressure) and biocarbon (6 mm diameter, 168 MPa pressure) pellets produced from spruce stem wood (1-2 mm particle size reacted at 320 ^{o}C and 12.4 MPa for 30 min) with 50 wt% liquid loading and different acetic acid content: (A) Tensile strength measured using diametric compression, (B) apparent density and (C) elasticity measurements as measured by volume expansion after 128 hrs following compression at 168 MPa

TPPB formation with rice straw

A series of tests were conducted to determine the effects of moisture content on the biochar properties of rice straw, a feedstock with 17% ash content. The initial test with rice straw (Table 2, Test ID 17) at 8.2% moisture content did not form TPPB under conditions which produced birch TPPB. Tests were conducted with 25, 50, 100, 150 and 225 wt% H_2O addition. Results from these tests show that TPPB formed with very high moisture content (150 wt% additional H_2O). Figures 5A and 5B present tensile strengths of rice straw biochar and biocarbon pellets as a function of moisture content. Biochar pellet tensile strengths displayed a linear dependence on water content increasing from 0.25 (25 wt% H_2O) to 0.45 MPa (225 wt% H_2O). Tensile strength of corresponding biocarbons showed a weaker trend (Figure 5B) varying from 4.5 MPa (≤100 wt% H_2O) to 6.5 MPa for the TPPC sample. All display tenfold increases in tensile strength upon calcination. Apparent densities of all the rice straw TPPC pellets were ~1.09 g/cc regardless of the initial moisture content used during the pyrolysis step.

Author Accepted Manuscript version of the paper by Robert L. Hohnson et al.
in Energy & Fuels, 37 (2023) Page 15808-15821,
http://dx.doi.org/10.1021/acs.energyfuels.3c01660

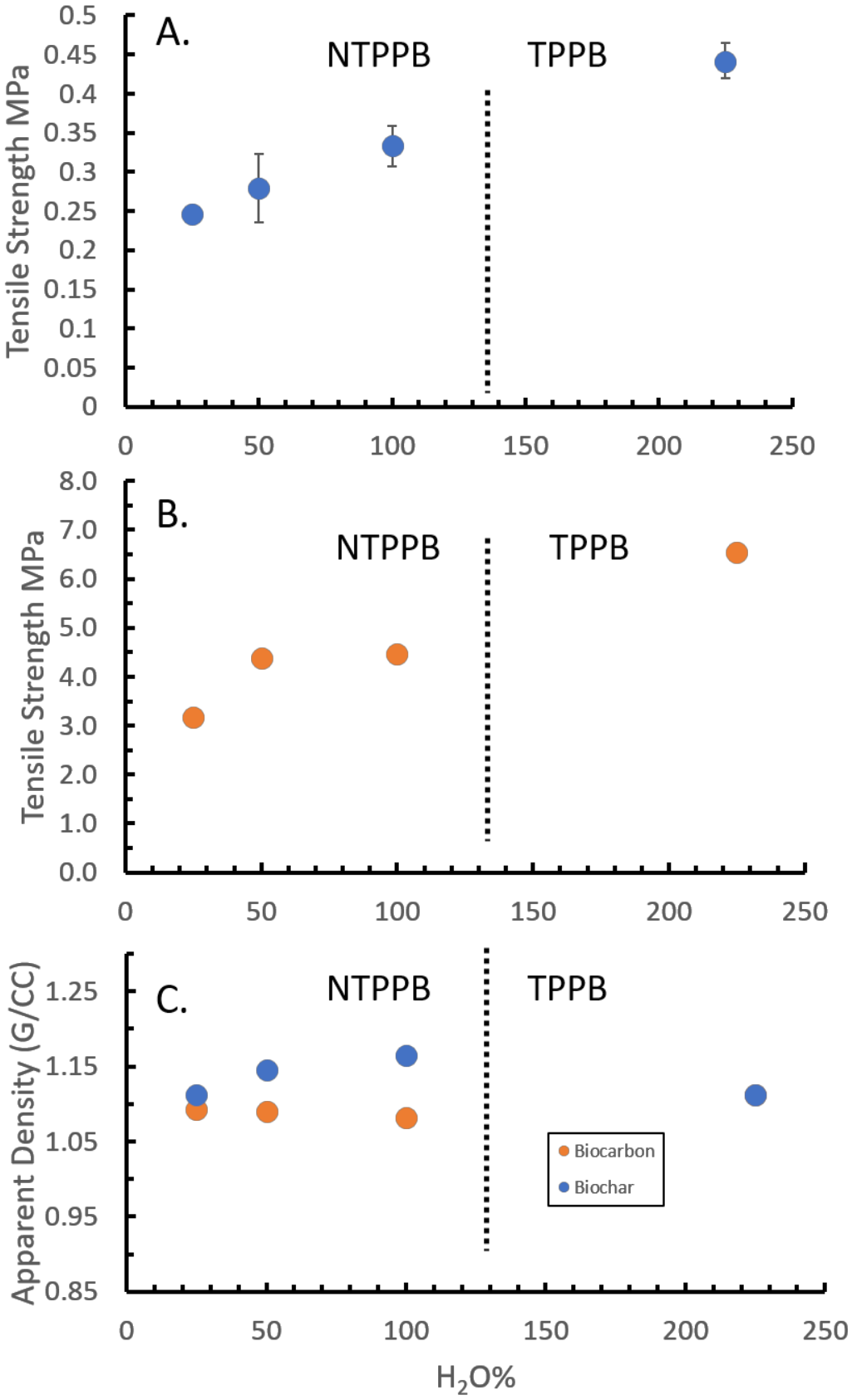

Author Accepted Manuscript version of the paper by Robert L. Hohnson et al.
in Energy & Fuels, 37 (2023) Page 15808-15821,
http://dx.doi.org/10.1021/acs.energyfuels.3c01660

Figure 5: Biochar (6 mm diameter, 88 MPa pressure) and biocarbon (6 mm diameter, 168 MPa pressure) pellets produced from rice straw (1-2 mm particle size reacted at 320 ^{o}C and 12.4 MPa for 30 min) for different % (wt) water added (A) Tensile strength as measured by diametric compression of biochar pellets, (B) Tensile strength of the biocarbon pellets following calcination (N_2) 900 ^{o}C, (C) Apparent density data for biochar and biocarbon pellets. 0 % and 150% water added sample data are not available.

The effect of moisture content on rice straw carbonization were explored using equilibrium analysis. Results of the equilibrium calculations are presented in Figure 6. Increasing moisture content from 0 to 28% reduces the solid carbon product (C(s)) (23.2 to 18.5 g) and increases the amounts of CO_2 and CH_4. These values remain level above 28% added moisture. Added moisture results in higher partial pressures of water in the gas phase, exhibited in three distinct ranges. The gas phase water content increases linearly with added moisture from 0 to 20%. The large amount of Si in the rice straw ash is largely present as SiO_2 below 20%, but hydrates to form H_2SiO_3 as added moisture increases from 20 to 24%. Above 26% added water, the reactor pressure stabilizes at 17.4 MPa, and further water addition results in an increasing mass of water in the liquid phase. Experimental reaction times do not approach equilibrium, but these results provide insight on how moisture partitions among products and the role that ash can play by binding water.

Author Accepted Manuscript version of the paper by Robert L. Hohnson et al.
in Energy & Fuels, 37 (2023) Page 15808-15821,
http://dx.doi.org/10.1021/acs.energyfuels.3c01660

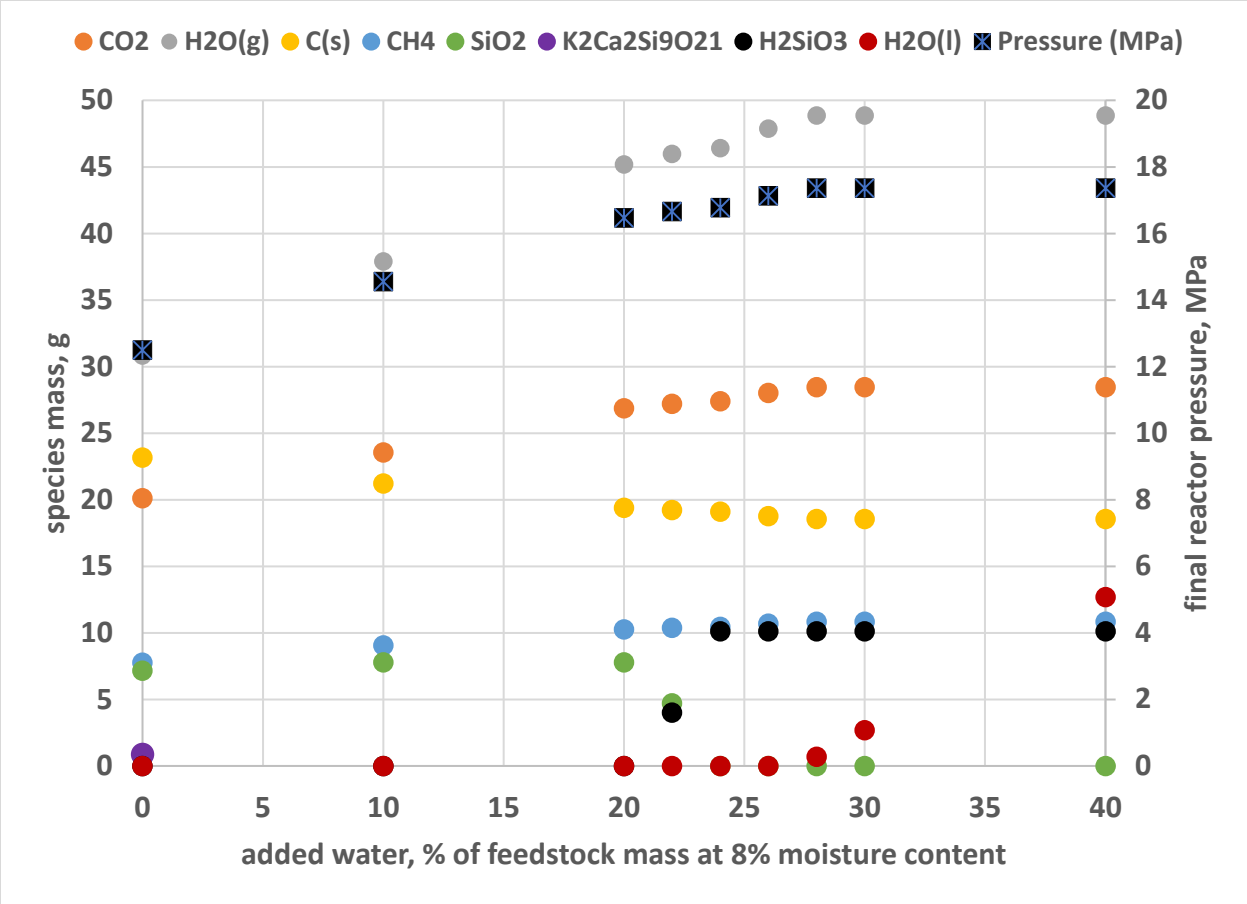

Figure 6. Results of equilibrium calculations of constant carbonization of rice straw at 320 °C as a function of added water.

TPPB from birch depressurized pyrolysis

Test ID 21 was conducted using birch with 25 wt% water added at 320 °C and 12.4 MPa constant pressure, conditions that formed TPPB as Test ID 15. After 20 min the pressure was slowly (<2 min) released from the system while the reactor remained in the sand bath for an additional 10 min, allowing water to boil off after TPPB had been formed. If these conditions did not produce TPPB with tensile strength comparable to Test ID 15, it would suggest that water remaining in the condensed phase is critical for maintaining the favorable properties of TPPB. A schematic of this process is shown in the Figure 7. Results show that despite forming TPPB, the particles plasticity was lost evident from the very low tensile strength of the biochar pellets formed. The biochar pellets did not have sufficient strength to meet minimum load cell force limits (>5 N). As expected, the biocarbon pellets also lacked sufficient strength to be tested,

Author Accepted Manuscript version of the paper by Robert L. Hohnson et al.
in Energy & Fuels, 37 (2023) Page 15808-15821,
http://dx.doi.org/10.1021/acs.energyfuels.3c01660

indicating that virtually no intra-particle bonding had occurred during calcination. This result strongly suggests that the water remaining in the condensed phase while at reaction temperature is critical for maintaining the improved plasticity (biochar) and reduced glass transition temperature needed for inter and intra particle bonding to produce strong biocarbons.

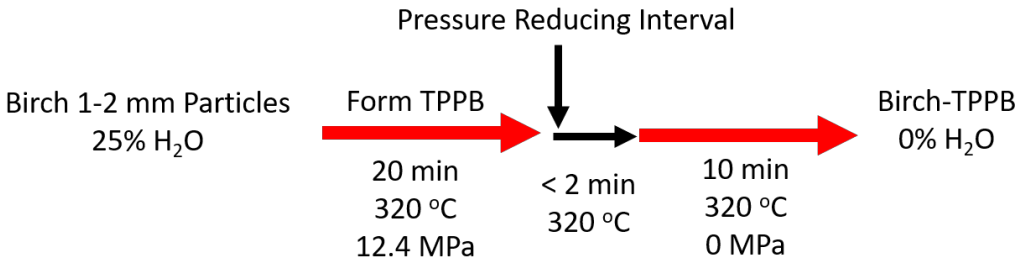

Figure 7. Reaction scheme for depressurized pyrolysis tests.

Results from TGA/DTG analysis comparing the depressurized sample to 25, 50, and 75 wt% water addition show a dramatic reduction in the mass loss between 200-300 °C and represent a loss of the reduced molecular weight fraction (Figure 8). As the overall char yield is only modestly reduced in the depressurized sample, (S1) which suggests the observed differences in the thermograms results from an increase in the average molecular weight of the remaining char. Furthermore, the reduction in mass loss between (200-300 °C) trends with increasing water addition supporting conclusions from pelletization experiments.

Author Accepted Manuscript version of the paper by Robert L. Hohnson et al.
in Energy & Fuels, 37 (2023) Page 15808-15821,
http://dx.doi.org/10.1021/acs.energyfuels.3c01660

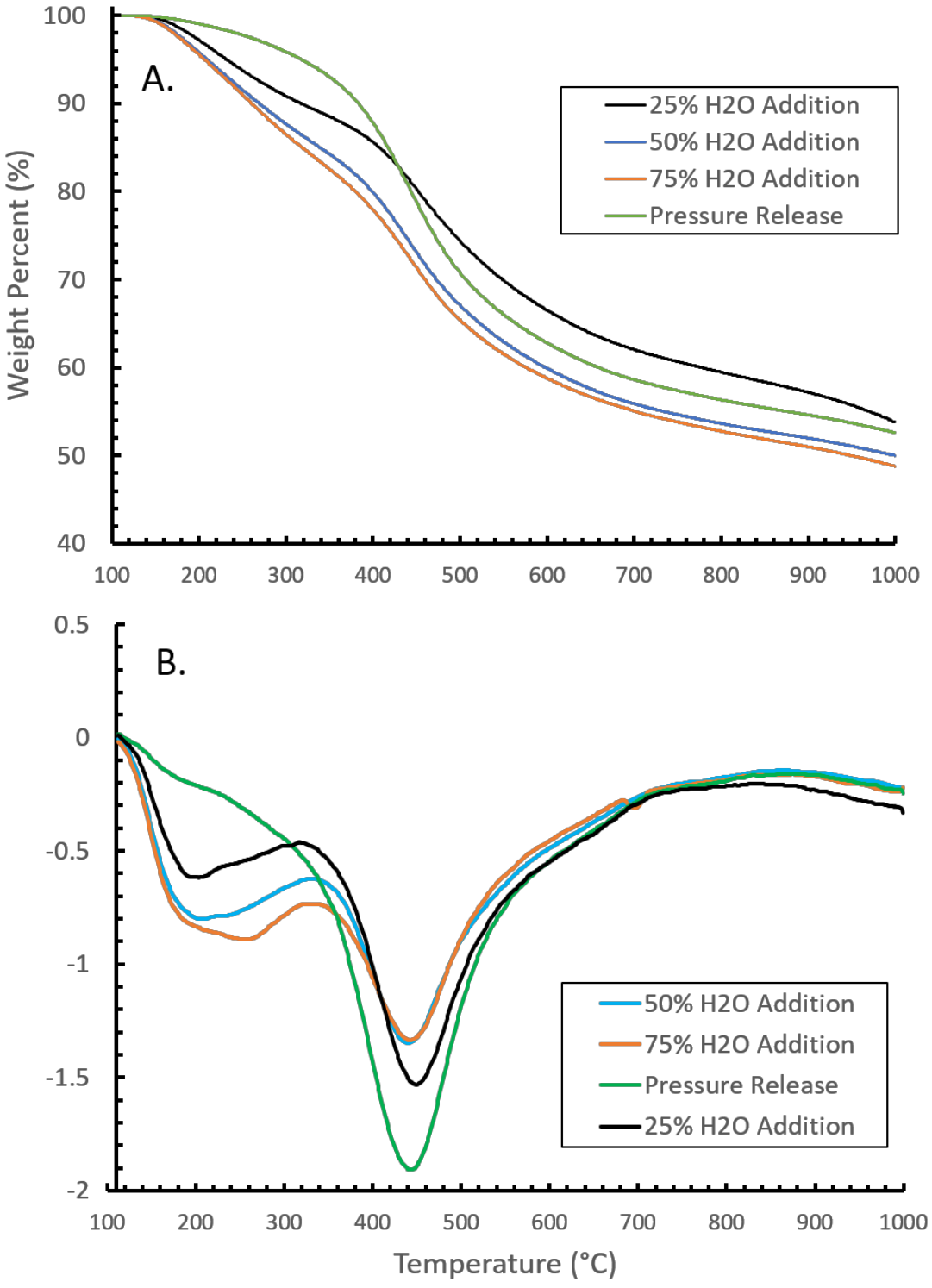

Author Accepted Manuscript version of the paper by Robert L. Hohnson et al.
in Energy & Fuels, 37 (2023) Page 15808-15821,
http://dx.doi.org/10.1021/acs.energyfuels.3c01660

Figure 8. TGA and DTG of birch stem wood biochar produced from (1-2 mm particle size produced at 320 °C and 12.4 MPa for 30 min) with different moisture contents, and with the pressure released while at reaction temperature.

Impact of particle size on mechanical properties of TPPC

Particle size is a critical variable that influences the mechanical strength of pellets formed from compression of particles, with smaller particles resulting is stronger pellets.[16, 19] Relatively large particles (0.5-1.0 mm) in a narrow size range were used in forming TPPB pellets discussed in previous sections above. To provide data comparable to commercial materials and literature values, birch and spruce TPPB samples (both produced at 320 °C, 12.4 MPa constant pressure, 75 wt% H_2O, and 30 min reaction time) were cryomilled to a fine powder prior to pellet formation and calcination. Apparent density, solid yield, tensile and compressive strength data are shown in Table 9. As expected, reducing the particle size resulted in a dramatic improvement in biocarbon pellet properties. Compared to the large particle data in Figure 1, pellets produced from finely ground birch had nearly 6X higher tensile strength (39.18 ±4 MPa), 20% higher apparent density (1.21 g/cm^3), and compressive strength (axial compression) of 188.75±31.6 MPa. Biocarbon pellets made from ground spruce TPPB showed a smaller improvement in the density and tensile strength as compared to birch. Compared to large particle data in Figure 3, the spruce biocarbon pellet density increased nearly 10% to 1.12 g/cc, the tensile strength quadrupled to 9.89 ±2.35 MPa and the compressive strength was 51.41± 18.7 MPa. Birch biocarbon tensile and compressive strength were nearly four times greater than that measured from spruce. Additionally, producing biocarbon using a TPPB intermediate increased the solid yield for birch and spruce from 20 to 32% and 23 to 35%, respectively, compared to direct pyrolysis of biomass. Raman spectroscopy was utilized to compare the graphitic character of the biocarbon pellets from birch and spruce Figure S1. The I(D)/I(G) (1350 cm^{-1}/1600 cm^{-1}) ratio provides a quantitative measure of the graphitic ordering of the carbon material.[30] The TPP Spruce 75% MC sample produced an I(D)/I(G) ratio of 1.46 with a G peak (1596.27) and a D peak (1346.41). The TPP Birch 75% MC sample produced an I(D)/I(G) ratio of 1.43 with a G peak (1581.72) and a D peak (1341.99). Both samples reflect a high disorder density as the I(D)/I(G) ratios are more significant than one.

Table 9: Mechanical properties calcined pellets from cryo-milled birch and spruce TPPB produced at 320 °C, 12.4 MPa constant pressure, 75 wt% H_2O, and 30 min reaction time

Material	Density (g/cc)	Tensile Strength (MPa)	Compressive Strength (MPa)	Solid Yield (Calcination)	Solid Yield (Total)
Birch	1.21+-.007	39.18+-4.05	188.75+-31.6	0.53+-0.002	0.32
Spruce	1.12 +-0.03	9.89+-2.35	51.41+-18.7	0.56+-.003	0.35
n	8	4	4	8	8

Author Accepted Manuscript version of the paper by Robert L. Hohnson et al.
in Energy & Fuels, 37 (2023) Page 15808-15821,
http://dx.doi.org/10.1021/acs.energyfuels.3c01660

The tensile and compressive strength values obtained are exceptionally high when compared to what is reported in the literature. The highest tensile strength of biochar pellets formed without a binder were produced via a hydrothermal carbonization. The process improved the tensile strengths of the feedstocks' pellets (1 to 3.9 MPa) to 3 to 7.5 MPa (hydrochar pellets).[31] Hydrothermal carbonization of waste wood at 200 °C and pH of 8 produced hydrochar pellets with slightly lower tensile strength, 2.5 MPa. .[32] These hydrochars were produced at relatively low temperatures (<250 °C) and the material structure would contain a very high oxygen content composed of furanics and arenes with little development of poly-condensed aromatic structures characteristic of well-developed coals or cokes.[33] Volatile matter contents of the hydrochars ranged from 50 to 75 %wt dry basis whereas TPPB samples were <50 %wt. Higher volumes of evolved gases during pellet calcination could affect its structural integrity. Results from calcination of steam exploded soft wood pellets showed tensile strength ranging from 2-3 MPa, depending on the calcination temperature.[34]

Bio-oil, starch, lignin and inorganic chemicals (i.e., NaOH) have been shown effective as binders to improve mechanical properties.. Strengths of 0.2 to 0.5 MPa were reported for pine biocarbon pellet utilizing bio-oil binder and as high as 4.4 MPa for pellets made from Norway spruce biochar, bio-oil, lignosulfonate, and water that were subsequently heated to 1,100 °C.[35-37] Rice husk biochar pellet tensile strengths (0.65 MPa) were improved using binders (3.8 to 24.5 MPa).[38] Rice husk contains ~16 wt% ash,[38] making it unsuitable for use in anodes., It is unclear how ash impacts the mechanical properties of the resulting biochars and biocarbons. Furthermore, the use of binders adds cost, and the resulting mechanical improvements is still not sufficient to meet specifications of petroleum derived materials.

Compressive strengths of CTP and calcined pet coke are typically 20-40 MPa depending on the CTP used, and the loading amounts.[1, 2] Biocarbon pellets produced from finely ground spruce TPPB did not show exceptionally high tensile (9.9 MPa) and compressive strengths (51.4 MPa), but are very high compared to values reported in the literature, and have compressive strength comparable to that of calcined CTP pet coke materials. The strongest non-engineered carbon materials are glassy carbons, which are produced from polymeric materials that experience a molten phase during carbonization (900-2000 °C),[39] but are non-graphitizable. Compression strength values for glassy carbons range from 200-800 MPa.[39] The biocarbon produced from birch has values approaching the lower end of the glassy carbon range. Higher TPPB calcination temperatures, currently untested, could result in a glassy carbon formation.

The pressurized pyrolysis conditions used in this study is a thermochemical transformation that is a hybrid between standard pyrolysis and hydrothermal carbonization (HTC), as the pressures used are sufficiently

Author Accepted Manuscript version of the paper by Robert L. Hohnson et al.
in Energy & Fuels, 37 (2023) Page 15808-15821,
http://dx.doi.org/10.1021/acs.energyfuels.3c01660

high to retain water in the condensed phase. Hydrothermal carbonization converts biomass submerged in hot compressed, sub-critical water at process temperatures of 180 to 260 °C yielding a product devoid of much of the hemicellulose present in the parent biomass.[40-42] This process is accelerated as compared to dry torrefaction as water reacts with the biomass surface resulting in solubilization of the hemicellulose and labile lignin components, which then are re-deposited onto the surface as seems as spheres with SEM. A key distinction between HTC and pressurized pyrolysis are the chemical processes that result in the transformation of the biomass material into a char product. During hydrothermal carbonization the main chemical driver leading to the transformation of the biomass material is the hydrolytic action of water, which at these temperatures behaves like an acid. This is evident as small particles lead to more rapid reactions in HTC,[43] whereas the TPPB molten phase is rapidly formed despite using large particles (2-4 mm), and larger parent biomass particles result in TPPB with better mechanical properties.[15] Products from HTC result from the break-down of labile components and re-deposition onto the materials in the form of droplets. TPPB under an SEM has the appearance of a totally amorphous solid without any morphological features of the parent material, with what looks to be pockets likely from the formation of gases in the melt.[15] The HTC thermal processes are not severe enough to break-down of much of the cellulose and lignin components, unlike pressurized pyrolysis in the temperature range used in this study. This is evident from the hydrochar retaining much of the morphological features of the parent biomass.[40, 44, 45]

Conclusions

This work reports the carbonization of different biomass materials under elevated and constant pressure conditions to investigate factors critical for the formation of transient plastic phase biochar (TPPB). The impacts of biomass type, water content, acetic acid, and reaction time were investigated. In additional to observing if a transient plastic phase occurred, the mechanical properties of biochars were further characterized using pelletization studies. Conditions of 12.4 MPa, 320 °C, ~8 %wt feedstock moisture content, and 30 minute reaction time produced TPPB from birch, oak, and avicell, but did not for spruce and rice straw. Increased moisture contents to 75 and 225 wt% of initial mass produced TPPB from spruce and rice straw, respectively. TPPBs formed from spruce and rice straw had improved mechanical properties, but not to the same degree observed with birch. Increasing birch moisture content near the

Author Accepted Manuscript version of the paper by Robert L. Hohnson et al.
in Energy & Fuels, 37 (2023) Page 15808-15821,
http://dx.doi.org/10.1021/acs.energyfuels.3c01660

water saturation point and reducing the reaction time to ~10 min further improved mechanical properties. In general, hardwood has higher tendency than soft wood to form TPPB, which is attributed to differences in lignin properties, in particular the reduced glass transition temperature of hardwood compared to softwood.[20] Maintaining pressure while at reaction temperature is critical to form a TPPB with improved material plasticity. Releasing the pressure slowly at reaction temperature flashes water from the condensed phase producing TPPB with extremely poor mechanical properties. Biocarbon produced from birch TPPB has the highest values of tensile and compressive strength reported in the literature, and exceeds mechanical strength benchmarks for aluminum electrodes and metallurgical reductants. Future work will focus on characterizing the porosity, reactivity and electrical resistivity of this material.

Acknowledgments:

The authors acknowledge the financial support from the Research Council of Norway and the BioCarbUp project industry partners: Elkem AS - Department Elkem Technology, Eramet Norway AS, Norsk Biobrensel AS, Eyde Cluster, Hydro Aluminium AS, and Alcoa Norway ANS. Additional support for the project was provided by the Office of Naval Research under grant number N-00014-18-1-2127.

Supporting Information: A summary table showing the biochar yield, fixed carbon content and biocarbon yield is supplied as Supporting Information

References:

(1) Hussein, A.; Picard, D.; Alamdari, H. Biopitch as a binder for carbon anodes: Impact on carbon anode properties. *ACS Sustain. Chem. Eng.* **2021,** 9, 4681-4687. doi: 10.1021/acssuschemeng.1c00618

(2) Couderc, P.; Hyvernat, P.; Lemarchand, J. L. Correlations between ability of pitch to penetrate coke and the physical characteristics of prebaked anodes for the aluminium industry. *Fuel* **1986,** 65, 281-287. doi: https://doi.org/10.1016/0016-2361(86)90022-0

(3) Xing, X.; Rogers, H.; Zhang, G.; Hockings, K.; Zulli, P.; Ostrovski, O. Coke degradation under simulated blast furnace conditions. *ISIJ International* **2016,** 56, 786-793. doi: 10.2355/isijinternational.ISIJINT-2015-704

(4) Xing, X.; Rogers, H.; Zhang, G.; Hockings, K.; Zulli, P.; Deev, A.; Mathieson, J.; Ostrovski, O. Effect of charcoal addition on the properties of a coke subjected to simulated blast furnace conditions. *Fuel Process. Technol.* **2017,** 157, 42-51. doi: https://doi.org/10.1016/j.fuproc.2016.11.009

(5) Xing, X.; Rogers, H.; Zulli, P.; Hockings, K.; Ostrovski, O. Effect of coal properties on the strength of coke under simulated blast furnace conditions. *Fuel* **2019,** 237, 775-785. doi: https://doi.org/10.1016/j.fuel.2018.10.069

(6) Patrick, J. W.; Stacey, A. E. The strength of industrial cokes: Part 3. Tensile strength of blast-furnace cokes. *Fuel* **1972,** 51, 206-210. doi: https://doi.org/10.1016/0016-2361(72)90082-8

(7) Antal, M. J.; Grønli, M. The art, science, and technology of charcoal production. *Ind. Eng. Chem. Res.* **2003,** 42, 1619-1640. doi: 10.1021/ie0207919

(8) Williams, S.; Higashi, C.; Phothisantikul, P.; Wesenbeeck, S. V.; Antal, M. J. The fundamentals of biocarbon formation at elevated pressure: From 1851 to the 21st century. *J. of Anal. Appl. Pyrolysis* **2015,** 113, 225-230. doi: 10.1016/j.jaap.2014.12.021

(9) Van Wesenbeeck, S.; Higashi, C.; Legarra, M.; Wang, L.; Antal, M. J. Biomass pyrolysis in sealed vessels. Fixed-carbon yields from avicel cellulose that realize the theoretical limit. *Energy Fuels* **2016,** 30, 480-491. doi: 10.1021/acs.energyfuels.5b02628

(10) Legarra, M.; Morgan, T.; Turn, S.; Wang, L.; Skreiberg, Ø.; Antal Jr, M. J. Carbonization of biomass in constant-volume reactors. *Energy Fuels* **2018,** 32, 475-489. doi: https://doi.org/10.1021/acs.energyfuels.7b02982

(11) Legarra, M.; Morgan, T.; Turn, S.; Wang, L.; Skreiberg, Ø.; Antal Jr, M. J. Effect of processing conditions on the constant-volume carbonization of biomass. *Energy Fuels* **2019,** 33, 2219-2235. doi: https://doi.org/10.1021/acs.energyfuels.8b03433

(12) Rios, R. V. R. A.; Martínez-Escandell, M.; Molina-Sabio, M.; Rodríguez-Reinoso, F. Carbon foam prepared by pyrolysis of olive stones under steam. *Carbon* **2006,** 44, 1448-1454. doi: 10.1016/j.carbon.2005.11.028

(13) Stahlfeld, K. W.; Belmont, E. L. Carbon foam production from lignocellulosic biomass via high pressure pyrolysis. *J. Anal. Appl. Pyrolysis* **2021,** 156, 105115. doi: 10.1016/j.jaap.2021.105115

(14) Lédé, J. Cellulose pyrolysis kinetics: An historical review on the existence and role of intermediate active cellulose. *J. Anal. Appl. Pyrolysis* **2012,** 94, 17-32. doi: 10.1016/j.jaap.2011.12.019

(15) Johnson, R. L.; Castillo, K.; Castillo, C.; Wang, L.; Skreiberg, Ø.; Turn, S. Q. Use of plasticized biochar intermediate for producing biocarbons with improved mechanical properties. *ACS Sustain. Chem. Eng.* **2023,** 11, 5845-5857. doi: 10.1021/acssuschemeng.2c05229

(16) Hiestand, E. N. Tablet bond. I. A theoretical model. *Int. J. Pharm.* **1991,** 67, 217-229. doi: https://doi.org/10.1016/0378-5173(91)90205-3

(17) Williams, O. A.-O.; Taylor, S.; Lester, E.; Kingman, S.; Giddings, D.; Eastwick, C. Applicability of mechanical tests for biomass pellet characterisation for bioenergy applications. *Materials* **2018,** 11, 1329-1347. doi:

(18) Sun, C. C. Decoding powder tabletability: Roles of particle adhesion and plasticity. *J. Adhesion Sci. & Tech.* **2011,** 25, 483-499. doi: 10.1163/016942410x525678

(19) Hilden, J.; Polizzi, M.; Zettler, A. Note on the use of diametrical compression to determine tablet tensile strength. *J. Pharm. Sci.* **2017,** 106, 418-421. doi: https://doi.org/10.1016/j.xphs.2016.08.004

(20) Suota, M. J.; da Silva, T. A.; Zawadzki, S. F.; Sassaki, G. L.; Hansel, F. A.; Paleologou, M.; Ramos, L. P. Chemical and structural characterization of hardwood and softwood lignoforce™ lignins. *Ind. Crops Prod.* **2021,** 173, 114138. doi: https://doi.org/10.1016/j.indcrop.2021.114138

Author Accepted Manuscript version of the paper by Robert L. Hohnson et al.
in Energy & Fuels, 37 (2023) Page 15808-15821,
http://dx.doi.org/10.1021/acs.energyfuels.3c01660

(21) Goring, D. A. I. Thermal softening, adhesive properties and glass transitions in lignin, hemicellulose and cellulose. *Trans. of the IIIrd Fund. Res. Symp. Cambridge* **1965,** 555-568. doi: DOI: 10.15376/frc.1965.1.555

(22) Babinszki, B.; Sebestyén, Z.; Jakab, E.; Kőhalmi, L.; Bozi, J.; Várhegyi, G.; Wang, L.; Skreiberg, Ø.; Czégény, Z. Effect of slow pyrolysis conditions on biocarbon yield and properties: Characterization of the volatiles. *Bioresour. Technol.* **2021,** 338, 125567. doi: https://doi.org/10.1016/j.biortech.2021.125567

(23) Cheng, Y.-S.; Zheng, Y.; Yu, C. W.; Dooley, T. M.; Jenkins, B. M.; VanderGheynst, J. S. Evaluation of high solids alkaline pretreatment of rice straw. *Appl. biochem. biotechnol.* **2010,** 162, 1768-1784. doi: 10.1007/s12010-010-8958-4

(24) Antal Jr, M. J.; Allen, S. G.; Dai, X.; Shimizu, B.; Tam, M. S.; Grønli, M. Attainment of the theoretical yield of carbon from biomass. *Ind. Eng. Chem. Res.* **2000,** 39, 4024-4031. doi: https://doi.org/10.1021/ie000511u

(25) Hyatt, J. A. Liquid and supercritical carbon dioxide as organic solvents. *J. Org. Chem.* **1984,** 49, 5097-5101. doi: https://doi.org/10.1021/jo00200a016

(26) Mellmer, M. A.; Sanpitakseree, C.; Demir, B.; Ma, K.; Elliott, W. A.; Bai, P.; Johnson, R. L.; Walker, T. W.; Shanks, B. H.; Rioux, R. M., et al. Effects of chloride ions in acid-catalyzed biomass dehydration reactions in polar aprotic solvents. *Nat. Commun.* **2019,** 10, 1132. doi: 10.1038/s41467-019-09090-4

(27) Johnson, R. L.; Perras, F. A.; Hanrahan, M. P.; Mellmer, M.; Garrison, T. F.; Kobayashi, T.; Dumesic, J. A.; Pruski, M.; Rossini, A. J.; Shanks, B. H. Condensed phase deactivation of solid brønsted acids in the dehydration of fructose to hydroxymethylfurfural. *ACS Catal.* **2019,** 9, 11568-11578. doi: 10.1021/acscatal.9b03455

(28) Trache, D.; Hussin, M. H.; Hui Chuin, C. T.; Sabar, S.; Fazita, M. R. N.; Taiwo, O. F. A.; Hassan, T. M.; Haafiz, M. K. M. Microcrystalline cellulose: Isolation, characterization and bio-composites application—a review. *Int. J. Biol. Macromol.* **2016,** 93, 789-804. doi: https://doi.org/10.1016/j.ijbiomac.2016.09.056

(29) Ying, W.; Fang, X.; Xu, Y.; Zhang, J. Combined acetic acid and enzymatic hydrolysis for xylooligosaccharides and monosaccharides production from poplar. *Biomass Bioenergy* **2022,** 158, 106377. doi: https://doi.org/10.1016/j.biombioe.2022.106377

(30) Ferrari, A. C.; Robertson, J. Interpretation of raman spectra of disordered and amorphous carbon. *Phys. Rev. B* **2000,** 61, 14095-14107. doi: 10.1103/PhysRevB.61.14095

(31) Liu, Z.; Quek, A.; Balasubramanian, R. Preparation and characterization of fuel pellets from woody biomass, agro-residues and their corresponding hydrochars. *Appl. Energy* **2014,** 113, 1315-1322. doi: https://doi.org/10.1016/j.apenergy.2013.08.087

(32) Wang, T.; Zhai, Y.; Zhu, Y.; Peng, C.; Xu, B.; Wang, T.; Li, C.; Zeng, G. Acetic acid and sodium hydroxide-aided hydrothermal carbonization of woody biomass for enhanced pelletization and fuel properties. *Energy Fuels* **2017,** 31, 12200-12208. doi: 10.1021/acs.energyfuels.7b01881

(33) Mao, J. D.; Johnson, R. L.; Lehmann, J.; Olk, D. C.; Neves, E. G.; Thompson, M. L.; Schmidt-Rohr, K. Abundant and stable char residues in soils: Implications for soil fertility and carbon sequestration. *Environ. Sci. Technol.* **2012,** 46, 9571-9576. doi: 10.1021/es301107c

(34) Wang, L.; Baldauf, L.; Skreiberg, O.; Jahrsengene, G.; Rørvik, S. Effect of calcination temperature and time on properties of steam exploded pellets. *Chem. Engin. Trans.* **2022,** 92, 355-360. doi: DOI: 10.3303/CET2292060

(35) Riva, L.; Nielsen, H. K.; Skreiberg, Ø.; Wang, L.; Bartocci, P.; Barbanera, M.; Bidini, G.; Fantozzi, F. Analysis of optimal temperature, pressure and binder quantity for the production of biocarbon pellet to be used as a substitute for coke. *Appl. Energy* **2019,** 256, 113933-113949. doi: https://doi.org/10.1016/j.apenergy.2019.113933

Author Accepted Manuscript version of the paper by Robert L. Hohnson et al.
in Energy & Fuels, 37 (2023) Page 15808-15821,
http://dx.doi.org/10.1021/acs.energyfuels.3c01660

(36) Riva, L.; Surup, G. R.; Buø, T. V.; Nielsen, H. K. A study of densified biochar as carbon source in the silicon and ferrosilicon production. *Energy* **2019,** 181, 985-996. doi: https://doi.org/10.1016/j.energy.2019.06.013

(37) Riva, L.; Wang, L.; Ravenni, G.; Bartocci, P.; Buø, T. V.; Skreiberg, Ø.; Fantozzi, F.; Nielsen, H. K. Considerations on factors affecting biochar densification behavior based on a multiparameter model. *Energy* **2021,** 221, 119893. doi: https://doi.org/10.1016/j.energy.2021.119893

(38) Hu, Q.; Shao, J.; Yang, H.; Yao, D.; Wang, X.; Chen, H. Effects of binders on the properties of bio-char pellets. *Appl. Energy* **2015,** 157, 508-516. doi: https://doi.org/10.1016/j.apenergy.2015.05.019

(39) Uskoković, V. A historical review of glassy carbon: Synthesis, structure, properties and applications. *Carbon Trends* **2021,** 5, 100116-100148. doi: https://doi.org/10.1016/j.cartre.2021.100116

(40) Bach, Q. V.; Skreiberg, O. Upgrading biomass fuels via wet torrefaction: A review and comparison with dry torrefaction. *Renew. Sust. Energ. Rev.* **2016,** 54, 665-677. doi: 10.1016/j.rser.2015.10.014

(41) Funke, A.; Ziegler, F. Hydrothermal carbonization of biomass: A summary and discussion of chemical mechanisms for process engineering. *Biofuels Bioprod. Biorefining.* **2010,** 4, 160-177. doi: 10.1002/bbb.198

(42) Libra, J. A.; Ro, K. S.; Kammann, C.; Funke, A.; Berge, N. D.; Neubauer, Y.; Titirici, M.-M.; Fühner, C.; Bens, O.; Kern, J., et al. Hydrothermal carbonization of biomass residuals: A comparative review of the chemistry, processes and applications of wet and dry pyrolysis. *Biofuels* **2011,** 2, 71-106. doi: 10.4155/bfs.10.81

(43) Reza, M. T.; Yan, W.; Uddin, M. H.; Lynam, J. G.; Hoekman, S. K.; Coronella, C. J.; Vásquez, V. R. Reaction kinetics of hydrothermal carbonization of loblolly pine. *Bioresour. Technol.* **2013,** 139, 161-169. doi: https://doi.org/10.1016/j.biortech.2013.04.028

(44) Sevilla, M.; Maciá-Agulló, J. A.; Fuertes, A. B. Hydrothermal carbonization of biomass as a route for the sequestration of co2: Chemical and structural properties of the carbonized products. *Biomass Bioenergy* **2011,** 35, 3152-3159. doi: https://doi.org/10.1016/j.biombioe.2011.04.032

(45) Xiao, L.-P.; Shi, Z.-J.; Xu, F.; Sun, R.-C. Hydrothermal carbonization of lignocellulosic biomass. *Bioresour. Technol.* **2012,** 118, 619-623. doi: https://doi.org/10.1016/j.biortech.2012.05.060

TOC Graphic

Author Accepted Manuscript version of the paper by Robert L. Hohnson et al.
in Energy & Fuels, 37 (2023) Page 15808-15821,
http://dx.doi.org/10.1021/acs.energyfuels.3c01660

Author Accepted Manuscript version of the paper by Robert L. Hohnson et al.
in Energy & Fuels, 37 (2023) Page 15808-15821,
http://dx.doi.org/10.1021/acs.energyfuels.3c01660